CIP Consolidated and Microwave Sintered Nanocrystalline Bulk TiNicu Shape Memory Alloy

M.M. RAJATH HEGDE, PRADEEP N B, SHANTHI KIRAN M

Abstract— TiNiCu alloy powder synthesized by mechanically alloying (MA) elemental powders exhibits metallic glass structure at longer ball milling duration. However, mechanical alloying due to ball milling duration of 50 hours indicates partial amorphous/nanocrystalline structure. Transition from elemental to ternary (NiCuO) and binary phases (TiNi, NiCu and tenorite) occur during ball milling process. Mechanically alloyed powders (75 hours of milling time) consolidated by cold isostatic pressing (CIP) showed partial transition from amorphous to crystalline structure during microwave sintering. Sintering process triggered the formation of intermetallic phases (Cu3Ti2 and Ni90Cu10O, TiNiCu, NiTi, Ni, Cu and CuNi), however crystallite size remained in the nanoscale regime. Unalloyed Ni and Cu crystallites were prevalent in the amorphous bulk TiNiCu glass. Transmission electron microscopy (TEM) characterization showed amorphous and crystalline structures during ball milling and consolidation respectively. During longer milling time B2 austenite and B19 (orthorhombic) martensite phases were formed as revealed by X-Ray Diffraction (XRD) investigation. During consolidation, stress and temperature induced transition of B2 to B19 (orthorhombic) and B19→B19' (Monoclinic) phase occurred revealing the susceptibility for shape memory effect (SME). Partial crystallization of amorphous phase into more stable TiNiCu (B19) martensite structure occurs during cooling cycle of microwave sintering.

Index Terms— Mechanical Alloying, TiNiCu, CIP, Shape Memory Alloys, XRD,TEM, Amorphous/Crystalline
.

1 INTRODUCTION

TiNi intermetallic compounds find wide range of applications as materials for engineering [1-4] and medical components [5-6]. Due to their abilities to exhibit shape memory behavior, biocompatibility and super elasticity, these compounds are suitable material for medical implants, as coil springs for actuators in micro electro mechanical devices, antenna, automobile, railway, eye glass frame and aerospace applications [7- 8]. Addition of Cu into binary TiNi could substitute Ni atoms which could lead to enhanced corrosion resistance, improved shape memory behavior and transformation characteristics [8-10]. Austenite (cubic) to martensite (B19 orthorhombic) and B19 (orthorhombic) to B19' (monoclinic) transformation is improved upon Cu addition [7-11]. TiNiCu alloys are traditionally synthesized by melting and casting, such a process has lot of disadvantages like evaporation, segregation, contamination, grain growth and handling of elevated temperature molten metal [12-15]. Mechanical alloying by high energetic ball milling is preferred in this research work mainly due to limitations of above mentioned process could be avoided. Moreover, alloying at ambient temperature, synthesis of nano sized crystallites, supersaturated solid solutions and amorphous phases is possible by this method [16]. Consolidation of nanostructured / amorphous / supersaturated solid solution powder into bulk solid form is a challenging task due to recrystallisation, grain growth and formation of ordered structure from non equilibrium phases and structure. In the recent past, there have been several research reports on consolidation of alloy powder by warm pressing, warm extrusion, hot pressing, explosive compaction and spark plasma sintering [17]. However, mechanically alloyed amorphous TiNiCu powder has not been consolidated by CIP compaction followed by microwave sintering technique. In this research work, we have chosen cold isostatic pressing followed by microwave sintering to produce bulk solid samples retaining the non equillibrium structures and phases.

2 Experimental Procedure

Elemental powders of Ti, Ni and Cu of purity 99.99 % is ball milled (Retsch PM 100) in an inert media at 200 rpm using tungsten carbide (WC) milling media with aball to powder weight ratio of 10:1. Milling was extended upto 75 hours of time, at a interval of every 10 hours, small quantity of milled powder was taken out for characterization.

Ball milled powders were consolidated by CIP using a liquid media of glycol mixed with water for applying pressure on powder. The powder is contained in a flexible mould and high pressure typically in the range of 200 to 400 MPa is applied to compress and form a green compact of high density capable of undergoing sintering.

X- Ray diffractometer (XRD) with a Cu Kα radiation (λ=0.1542 nm) was used to examine the structural parameters of samples during MA and CIP consolidated microwave sintered bulk samples. Bragg's and Scherrer's equations allow determination of overall structural parameters, such as lattice parameter (*a*), crystallite size (*D*, average coherently diffracting domain size) and microstrain. Crystallite size (D) was calculated using the Scherrer formula, $D = 0.94\lambda/\beta\cos\theta$, where λ is the wavelength of the incident radiation (X-ray) and β is the full width at half maximum and also using xpert high score plus software profile fitting.

The powder sample (nanoparticles) is dispersed in ethanol solution using ultrasonication for five minutes.

The solution used evaporate in a reasonable time (in about 10-20 minutes) at room temperature. The suspended particles are lifted on a carbon-coated copper grid (of 200 or 300 mesh) with the help of forceps, by dipping the grid gently in the solution. The grid is dried on a filter paper under an infrared lamp, followed by inspection in the TEM. Thus, structure of the samples were evaluated by XRD and TEM (SADP).

Electromagnetic spectrum of frequency used in microwave sintering is 2.45 GHz and 915 MHz frequencies. Alloy powders are good absorbers of microwaves and heat (500^0 C) up rapidly at a heating rate as high as 100^0 C/min. Ball milling has resulted in very fine particle size, increased surface area leading to higher energy in the powder due to strain hardening. These factors facilitate atomic mobility during sintering triggering rapid densification as shown in figure 1.

3 Results and Discussion

3.1 XRD Characterisation of as Milled Powder as a Function of Milling Time

XRD pattern of unmilled mixture of elemental powder is shown in Fig. 2, elemental bragg peaks of TiO, Ni, and Cu are visible. Peaks are narrow, symmetrical with high relative intensity indicating a complete **crystalline** phase. Quantitative analysis indicates the relative percentage of each phase and structural parameter of the unprocessed powder mixture is given in Table I. Prominent peak (101 TiO) among the diffraction peaks has a full width half maximum (FWHM) value of 0.1301^0, indicating a very narrow peak with high counts (44090.83) and relative intensity of 100 %. Crystallite size (D) of unmilled powder mixture was found to be in the range of 60 µm.

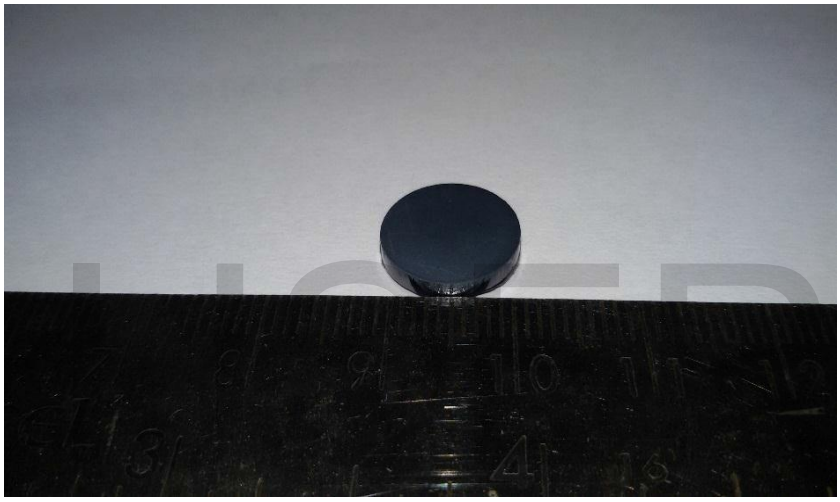

Fig. 1 CIP consolidated microwave sintered bulk disc from 75 hours ball milled powder

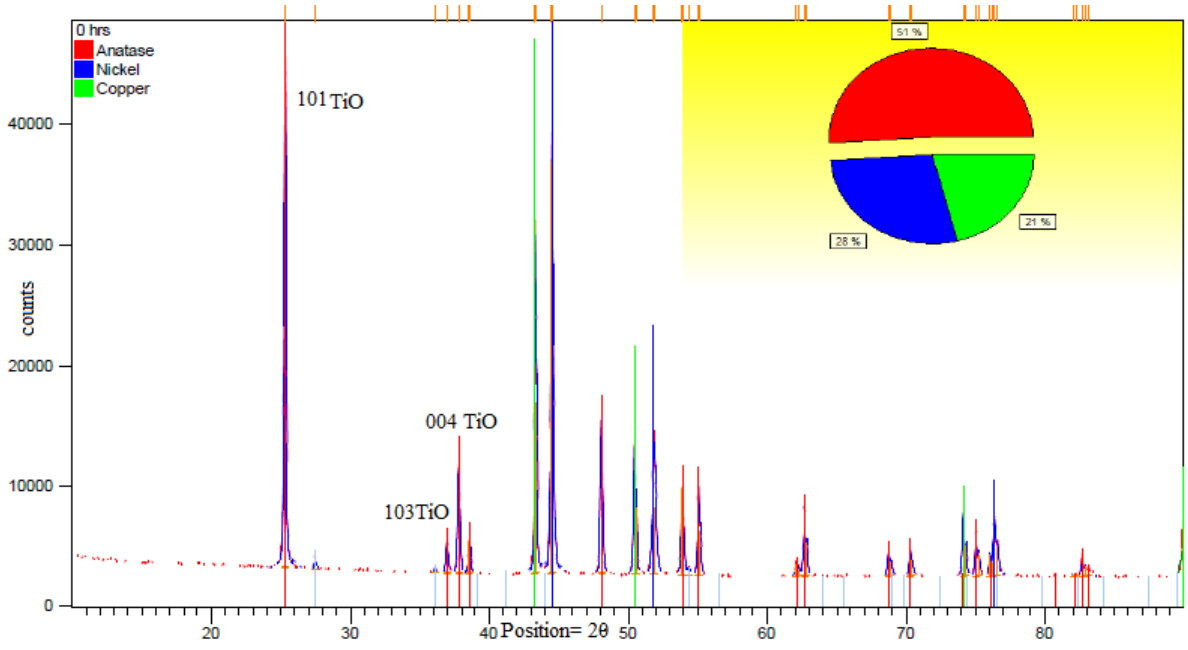

Fig. 2 XRD pattern of unmilled mixture of elemental powders

TABLE I
STRUCTURAL PARAMETERS OF ELEMENTAL POWDERS (UNPROCESSED)

Pos. [°2Th.]	Phase	FWHM [°2Th.]	d-spacing [Å]	Rel. Int. [%]	'D' nm
25.2965	TiO/Ni	0.1301	3.51791	100.00	
37.7797	TiO	0.1420	2.37930	19.83	60 um
43.3117	Cu	0.1036	2.08736	63.93	
44.4877	Ni	0.1541	2.03487	77.59	

As milling duration of elemental powder increases to 10 hours, Cu_3Ti, NiTi and NiCuO solid solution is formed by the mechanism of diffusion as indicated by the XRD Bragg peaks in figure 4. Solid solution was formed by ballistic diffusion of Cu and Ni atoms into the crystal structure of Ti during MA. Further, Cu and O atoms diffused into the crystal structure of Ni forming NiCuO. Elemental phases of Cu and Ni along with anatase phase are visible indicating the presence of unalloyed elemental phases. Structural parameters in table II shows XRD peak broadening (FWHM = 0.5077^0) and shifting of Bragg peaks. Broadening indicates the phenomenon of crystallite size (79.6 nm) refinement and increased lattice strain (0.332 %) [18]. Shifting of diffraction peaks to higher Bragg angle (2θ) is a phenomenon related with the formation of new phases (NiCuO, CuTi and NiTi solid solutions) [18]. Atomic radii of Cu (0.128 nm) and Ni (0.125 nm) are almost identical and that of Ti (0.147 nm) is larger, thus Cu is more likely to diffuse into Ti rather than Ni crystal structure.

Cu_3Ti is orthorhombic, NiTi is monoclinic and $Ni_{0.85}Cu_{0.15}$ O is FCC in crystal structure. Intensity of almost all the peaks (ex, peak of $2\theta=25.6094^0$ is 2266.09 cts) in terms of height have been drastically reduced compared to unmilled elemental powder. Interesting phase transformations are observed with the formation of Ti from TiO, while O has diffused out of TiO forming NiO_2 (monoclinic) and NiCuO. CuNi (FCC), NiO_2 and Cu_2O (cuprite of BCC structure) are the new phases formed during ball milling duration of 20 hours. TiO (anatase), along with elemental Cu and Ni exists after 30 hours of milling time indicating the presence of unalloyed phases. Remaining phases are indicated in the XRD pattern in Figure 4. Due to continuous collision energy of the balls on the powder sample, Further peak broadening ($0.9646\ ^0$) and reduced counts/intensity (1494.46 ht) are observed from Table III indicating the process of crystallite size (15.2 nm) refinement, increased lattice strain (0.934 %) and decline in crystallinity are observed during 30 hours of MA. Cu and Ni phases are diminishing as a consequence of alloying.

TABLE II
STRUCTURAL PARAMETERS OF ELEMENTAL POWDERS MA FOR 10 HOURS OF BALL MILLING DURATION

Pos. [°2Th.]	Height [cts]	FWHM [°2Th.]	d-spacing [Å]	Rel. Int. [%]	'D' nm / lattice strain %
25.6094	2266.09	0.4102	3.47563	100.00	
44.7692	1211.92	0.5077	2.02273	53.48	79.6/0.332
48.3168	1572.70	0.3561	1.88217	69.40	

TABLE III
STRUCTURAL PARAMETERS OF ELEMENTAL POWDERS MA FOR 30 HOURS OF BALL MILLING DURATION

Pos. [°2Th.]	Height [cts]	FWHM [°2Th.]	d-spacing [Å]	Rel. Int. [%]	'D' nm / Lattice strain %
25.4459	3293.22	0.3086	3.49759	100.00	
44.6345	1494.46	0.9646	2.02852	45.38	15.2/0.934
48.1681	1482.75	0.2745	1.88763	45.02	

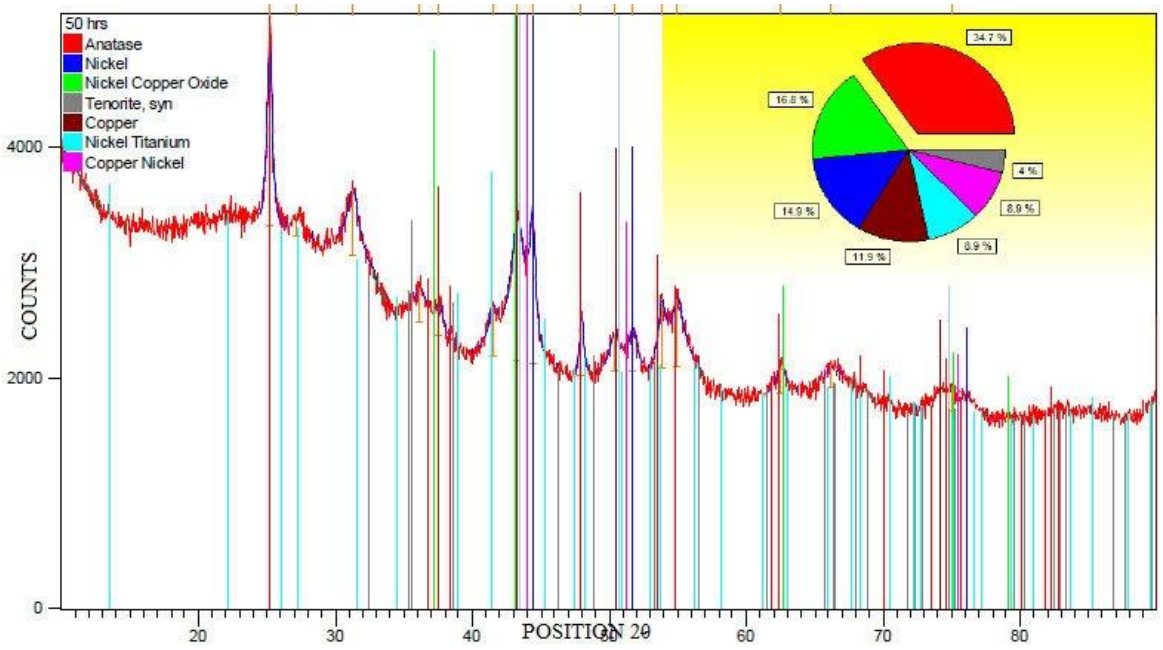

Fig. 3 XRD pattern of ball milledpowder as a function of 50 hours of milling time

There is a huge decrease in the height (1200 to 1500 cts) of all the diffracted peaks and a large increase in their width (FWHM = 1.3803^0) indicating the process of transition from a crystalline phase to amorphous, crystallite refinement, alloying and increased strain during the course of MA. Crystallite size and lattice strain obtained at this juncture (50 hrs) of milling (MA) duration are 8.7 nm and 1.452 % respectively as indicated in Table IV. Anatase XRD peak (101) is reduced drastically in height, Cu is almost vanished as a consequence of MA phenomenon which has caused the formation of Copper oxide (Tenorite, represented in gray color) and NiTi (sky blue color) binary solid solutions of non-equilibrium nature. In addition to these phases, NiCuO and CuNi phases are prevalent as observed from XRD pattern in figure 3. According to quantitative analysis in figure 3 and table IV, stress induced martensite (B19) and austenite (B2) phases are observed. Such phases have emerged due to severe plastic deformation, increased temperature during continuous collision of balls with powder causing strain energy [16].

Figure 4 shows the X-ray diffraction pattern of elemental powder MA for 75 hours of ball milling duration, no crystalline peaks are seen which indicates fully amorphous (Ti (Ni Cu) alloy glass) powders were formed. There are several factors related to amorphization of mechanically alloyed powder, few important ones are milling time, alloying system, and amorphization reactions such as continuous peak broadening, peak shifting and crystallite size refinement. All these reactions have been reported in XRD and TEM characterization results in this research article.

TABLE IV
STRUCTURAL PARAMETERS OF ELEMENTAL POWDERS MA FOR 30 HOURS OF BALL MILLING DURATION

Pos. [°2Th.]	Height [cts]	FWHM [°2Th.]	d-spacing [Å]	Rel. Int. [%]	'D' nm/ lattice strain %/phase
25.1938	1588.04	0.4615	3.53202	100.00	
37.5294	275.85	0.7800	2.39460	17.37	B 19 martensite 110
43.3037	1233.90	1.3803	2.08773	77.70	8.7/1.452
44.3536	1310.09	0.5141	2.04071	82.50	B2 austenite 110
47.9408	484.17	0.3468	1.89605	30.49	B 19 martensite 020

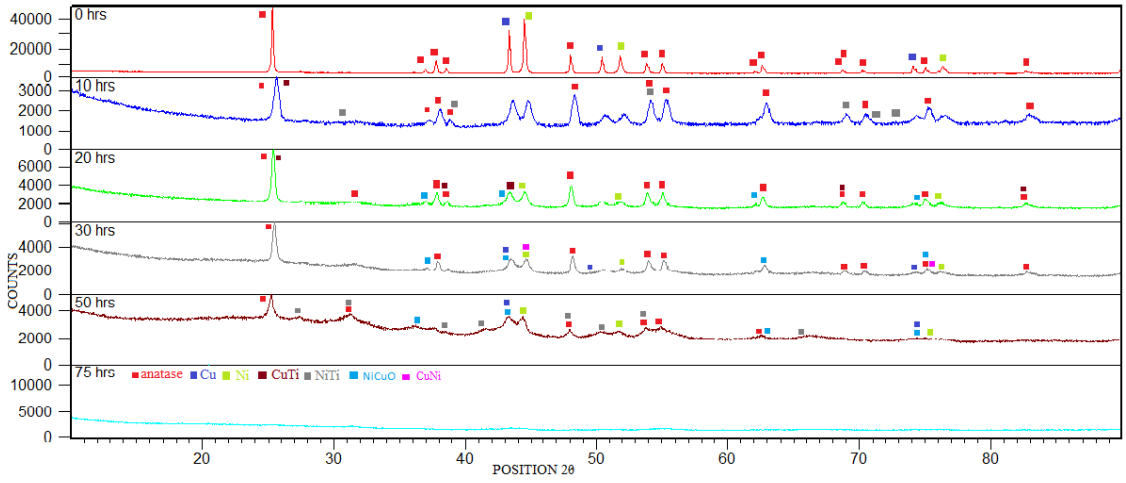

Fig. 4 XRD pattern of as-milled powders as a function of milling time

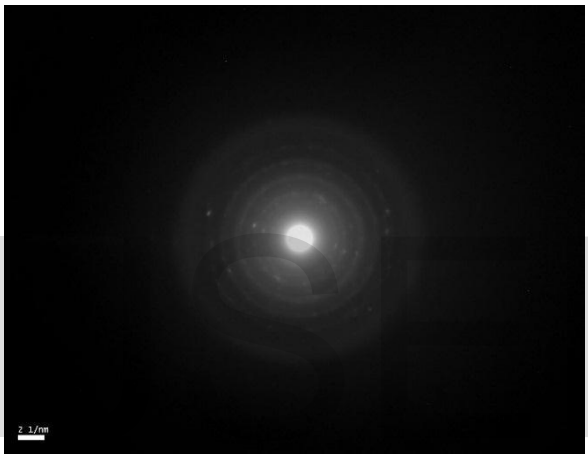

Fig. 5 Selected Area Diffraction Pattern (SADP) for 75hrs of ball milled powder sample

3.2 Transmission Electron Microscopy (TEM) of milled powder

Electron diffraction rings are too diffused to permit identification of crystals, no continuous polycrystalline rings are visible, fully amorphous halo pattern of SAD pattern is observed in figure 5. Such a pattern suggests almost an amorphous phase in the powder subjected to 75 hours of milling time.

3.3 XRD Characterisation of CIP Consolidated Bulk Compacts (Disc)

XRD pattern of bulk compact (disc) synthesised by CIP consolidation followed by microwave sintering from 30hrs of mechanical alloyed powder is shown in figure 6 and its structural parameters are given in table V. Anatase phase is the major composition among the other ingredients like inter-metallic phase of TiNiCu, Cu_3Ti_2, NiTi, Ni, Cu, CuNi and $Cu_{10}Ni_{90}O$. XRD peak narrowing, shifting and increased intensities (Peak 2θ=25.3493^0, FWHM=0.1 to 0.9^0 and Height=6411 cts) are noted. Significance of peak narrowing are crystallite size (64.2nm) growth and decreased lattice strain (0.377%) as a consequence of elevated sintering temperature and shifting of Bragg peaks initiates the formation of new phases. XRD pattern in figure 6 reveals partial crystallization of amorphous structure during microwave sintering. The structural parameters (table VI) indicate broader peaks (FWHM is 0.5 to 1.6^0), nano sized (7 nm) crystallites and the presence of intermetallic compounds. It has been reported that the enthalpy (ΔH= 140 kJ/mol) required for the formation of TiNiCu (B19′) is stronger than that required for NiTi (ΔH= 67 kJ/mol) and CuTi [19]. Moreover, the Gibbs free energy of TiNiCu is much lower than that of NiTi and CuTi goes to suggest its stable formation [19]. Prevalence of B19′ monoclinic phase is evident and attributed to the partial transition of B2 to B19′ during the cooling cycle and the transition temperature is well above room temperature. Stress and temperature induced B2 to B19 and B19→B19′ transition indicates the susceptibility of shape memory effect.

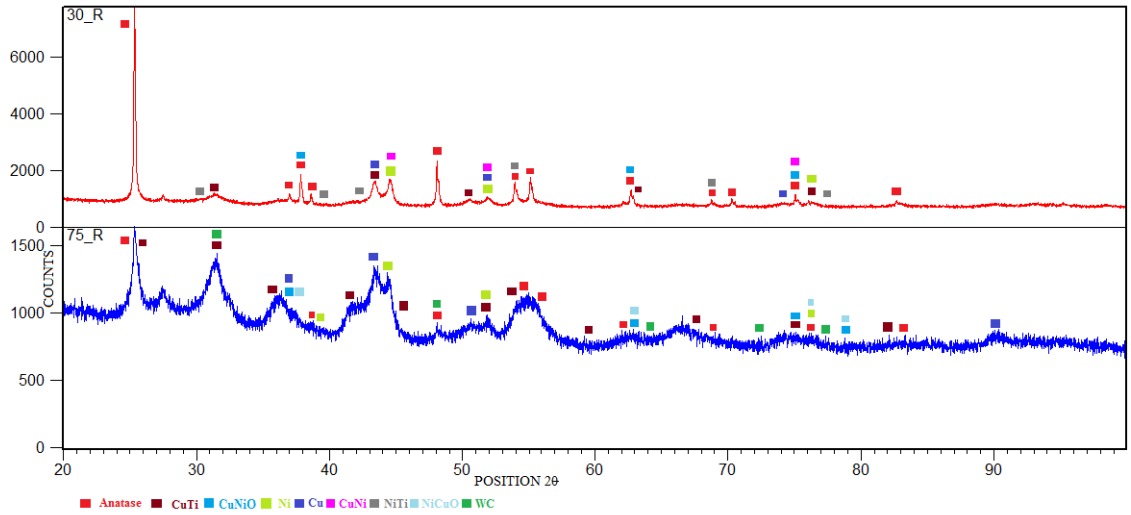

Fig. 6 XRD pattern of CIP consolidated microwave sintered discs as a function of milling time

TABLE V
STRUCTURAL PARAMETERS OF CIP CONSOLIDATED MICROWAVE SINTERED DISC FROM 30 HOURS MILLING TIME

Pos. [°2Th.]	Height [cts]	FWHM [°2Th.]	d-spacing [Å]	Rel. Int. [%]	'D' nm/ lattice strain %
25.3493	6411.39	0.1315	3.51070	100.00	
37.8400	1005.88	0.1160	2.37565	15.69	B19 Martensite
38.6108	335.92	0.1071	2.32998	5.24	
41.7018	126.16	0.9363	2.16414	1.97	B19 Martensite
43.4059	686.00	0.9344	2.08304	10.70	B2 Austenite
44.5008	826.06	0.5336	2.03430	12.88	64.2/0.377/B19 Martensite
48.0798	1427.08	0.1289	1.89089	22.26	B19 Martensite

TABLE VI
STRUCTURAL PARAMETERS OF CIP CONSOLIDATED MICROWAVE SINTERED DISC FROM 75 HOURS MILLING TIME

Pos. [°2Th.]	Height [cts]	FWHM [°2Th.]	d-spacing [Å]	Rel. Int. [%]	'D' nm/lattice strain %
25.3836	517.71	0.6357	3.50604	100.00	
41.6423	237.05	0.8767	2.16710	45.79	B19 Martensite
43.4846	454.74	1.6825	2.07946	87.84	6.7/1.789 B2 Austenite
44.4730	418.75	0.5026	2.03551	80.89	B19 Martensite
48.0771	57.57	0.2463	1.89100	11.12	B19 Martensite

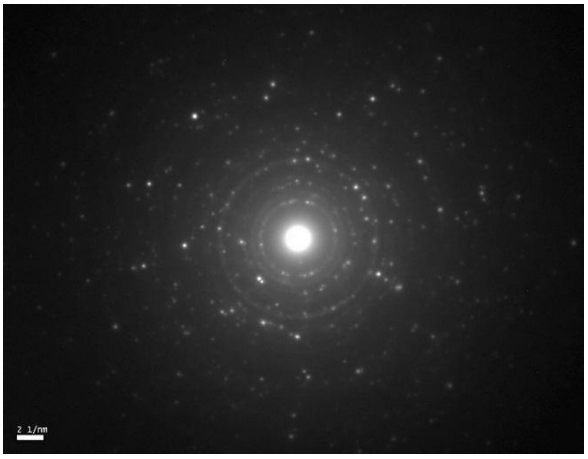

Fig.7 SADP of CIP consolidated microwave sintered disc from 75 hours milling time

3.4 Transmission Electron Microscopy (TEM) of CIP Consolidated Bulk Compact (Disc)

Few nanocrystals which were prevalent in the 75 hours ball milled powder have acted as pre-existing nuclei for recrystallisation process during microwave sintering thus reducing the crystallization temperature. Thus, a more pronounced bright sparkling crystallites are visible in the TEM SAD pattern shown in figure 7 which indicates crystalline structure. However, the diffractions rings are still diffused to allow identification of crystals which goes to show the existence of partial amorphous structure.

4 CONCLUSIONS

Ball milling has resulted in vanishing of elemental phases and crystallite size reduction to nano size regime (< 50 nm). Cu_3Ti and NiTi have formed during ball milling durations of 50 hours with oxygen contamination resulting in NiCuO formation. In addition, CuNi and NiO_2 are formed at the end of 50 hours of ball milling duration. B2 (cubic) and B19 (orthorhombic) phases are formed during prolonged milling time of ≥ 30 hours due to severe plastic deformation, temperature increase due to collision of balls and strain energy. Amorphous with slight crystalline structure is obtained at the end of 75 hours of milling time for Ti(NiCu) which is the lone phase existing. Intermetallic compounds of TiNiCu, Cu_3Ti_2, NiTi and CuNi are formed during microwave sintering of CIP consolidated disc. Recrystallisation has occurred during elevated temperature consolidation with slight grain growth, however traces of amorphous regions are noted. Traces of elemental Ni and Cu are observed in the microwave sintered disc. Stress, temperature and strain induced transition of B2→B19 and B19→B19′ phase is noted indicating the susceptibility of shape memory effect. Enthalpy of TiNiCu formation is high while the free energy is lowest indicating the most stable phase.

ACKNOWLEDGEMENT

We would like to thank CMTI Bangalore and SAIF IITB Mumbai for providing CIP, XRD and TEM facilities and also we are grateful to the department of materials and metallurgical at NITK Surathkal for providing ball milling and microwave sintering facilities.

REFERENCES

1. Humbeeck JV. Non-medical applications of shape memory alloys. *Mater. Sci. Eng A* 1999;273-275:134–48.
2. Stoeckel D. Shape memory actuators for automotive applications. *Mater. Des 1990*;11(6):302–7.
3. Predki W, Knopik A, Bauer B. Engineering applications of NiTi shape memory alloys. *Mater. Sci. Eng A* 2008;481-482:598–601.
4. Huang W. On the selection of shape memory alloys for actuators. *Mater. Des* 2002;23:11–9
5. Pelton AR, Stöckel D, Duerig TW. Medical uses of nitinol. *Mater. Sci. Forum* 2000;327–328:63–70.
6. Thompson SA. An overview of nickel–titanium alloys used in dentistry. *Int. Endod. J* 2000;33:297–310.
7. Otsuka K, Ren X. Physical metallurgy of Ti–Ni based shape memory alloys. *Prog Mater Sci* 2005;50:511–678.
8. Lagoudas DC. Shape memory alloys modeling and engineering applications. *Texas: Springer*; 2008.
9. Haider W, Munroe N, Pulletikurthi C, Singh Gill PK, Amruthaluri S. Comparative biocompatibility analysis of ternary nitinol alloys. *J Mater Eng Perform* 2009;18:760–4.
10. Phukaoluan A, Khantachawana A, Kaewtatip P, Dechkunakorn S, Anuwongnukroh N, Santiwong P, et al. Property improvement of TiNi by Cu addition for orthodontics applications. *Appl Mech Mat* 2011;87:95–100.
11. Potapov PL, Shelyakov AV, Schryvers D. On the crystal structure of TiNi–Cu martensite. *Scr Mater* 2001;44:1–7.
12. Van Loo FJJ, Bastin GF, Leenen AJH. Phase relations in the ternary Ti-Ni-Cu system at 800 and 870 C. *J Less-Common Met* 1978;57:111–21.
13. Fukuda T, Saburi T, Chihara T, Tsuzuki Y. Mechanism of B2– B19-B19′ transformation in shape memory Ti–Ni–Cu alloys. *Mater Trans* 1995;36:1244–8.
14. Lin K, Wu S. Multi-stage transformation in annealed Ni-rich Ti49Ni41Cu10 shape memory alloy. *Intermetallics* 2010;18:87– 91.
15. Rozner AG, Heintzelman EF, Buehler WJ, Gilfrich JV. Effect of addition of oxygen, nitrogen and hydrogen on microstructure andhardness of cast TiNi intermetallic compound. *Trans ASM* 1965;58:415–8.
16. Suryanarayana C, Klassen T, Ivanov E. Synthesis of nanocomposites and amorphous alloys by mechanical alloying. *J Mater Sci* 2011;46:6301–15.
17. Inoue A, "Amorphous, nanoquasicrystalline and nanocrystalline alloys in Al-based systems." *Progress in Materials Science*, vol. 43, no. 5, pp. 365–520, 1998.
18. Fatemeh Alijani, Rasool Amini et al, Effect of milling time on the structure, micro-hardness, and thermal behavior of amorphous/nanocrystalline TiNiCu shape memory alloys developed by mechanical alloying. *Materials and design* 2014; 55: 373-380.
19. Locci AM, Orru R, Cao G, Munir ZA. Field-activated pressure- assisted synthesis of NiTi. *Intermetallics* 2003;11:555–71.